

# Back-projection imaging of physically-modelled seismic data

Joe Wong and Kevin W. Hall

## ABSTRACT

Full waveform inversion (FWI) is a technique that yields high resolution images from measured wavefields of the underlying velocity/density structure. However, FWI depends on iterative forward modelling of wave propagation through complex structures. FWI can be very inefficient and time consuming if the starting model is not close to the true model because of the many more iterations required. This issue is made worse if the measured data has low SNR. One way of significantly reducing the number of iterations needed and thus speeding up the FWI process is to have a starting model that is close to the actual model in terms of location, size, and shape. We recorded transmission seismograms across a 2D region containing isolated targets, and used iterative back-projection of travel-time and amplitude anomalies to create such starting models.

## INTRODUCTION

FWI depends on iterative forward modelling of wave propagation through complex structures. When forward modelling done using (time- or frequency-domain) finite difference methods, a good starting structure close to the real underlying structure must be defined on a gridded space. The gridded space must have many cells whose sizes must be equal to or less than about 1/8 the dominant wavelength of the source wavelet. Because of the large number of cells on which the velocity/density structure is defined, and because many iterations are required to achieve an acceptable result, FWI can be very time-consuming if the starting model is not close to the true structure. This issue is made worse if the measured data has low signal-to-noise ratios (SNRs).

One way to decrease the iterations needed to find an acceptable FWI version of the true structure is to start with an estimate that is close to the true structure. We believe that iterative back-projection of observed first-arrival times (or first-arrival amplitudes corrected for geometric spreading) is a fast and efficient way of creating such a good estimate. We conducted physical modelling surveys recording transmission seismograms across a 2D area with isolated targets to obtain experimental on which to test this belief.

## BACK-PROJECTION METHOD

The first step in the back-projection method is to define a grid of rectangular cells that cover the scanned region (see Figure 1). Using the coordinates of the source and receivers associated with a particular observed seismogram, we can draw a straight ray for this seismogram. Using the observed first arrival time  $t_k^{obs}$  and the length  $l_k$  of the  $k$ -th ray, we find the average value of slowness:

$$u_{avg} = \sum_{k=1}^M (t_k^{obs} / l_k) / M \quad . \quad (1)$$

where  $M$  is the number of rays. The value  $u_{avg}$  is then assigned to every cell with at least one ray crossing. We then determine the ray segment length  $\Delta l_{ki}$  in cell  $i$  crossed by ray

$k$ . This requires finding the intersections of the ray  $k$  with cell boundaries, as shown on Figure 1(b). The following is then true:

$$l_k = \sum_{i=1}^N (\Delta l_{ki}) \quad , \quad (2)$$

where  $N$  is the total number of cells (if ray  $k$  does not cross cell  $i$ , then  $\Delta l_{ki}$  is zero).

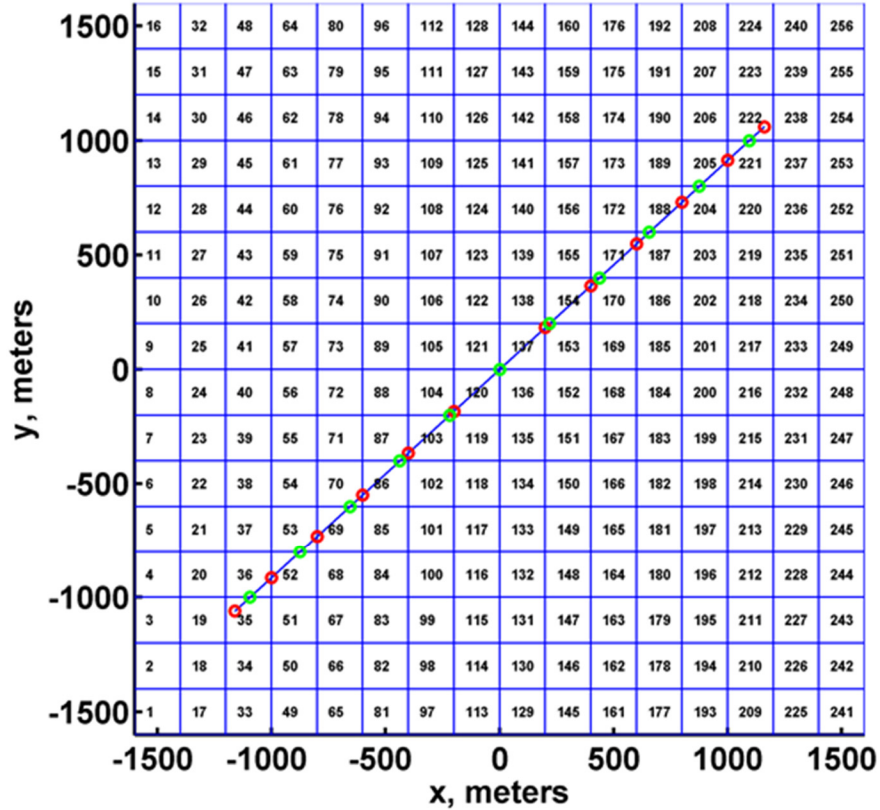


FIG. 1. An example grid of cells defining the scanned region. Cell sizes are 100m by 100m; the number of cells in both the X and Y directions is 16. The cells are numbered up along columns. One ray is drawn, showing its intersections with cell boundaries.

At this first step of iterative back-projection,  $u_i = u_{avg}$  fills the cells  $i$  crossed by at least one ray. Then, for each ray, a calculated arrival time is found by summing the products of cell slownesses and cell ray segment lengths:

$$t_k^{cal} = \sum_{i=1}^N (\Delta l_{ki} * u_i) \quad (3)$$

Many of the segment lengths  $\Delta l_{ki}$  are zero. For each ray  $k$ , and each cell  $i$ , we then find

$$\Delta u_{ki} = f_{ki} * (t_k^{obs} - t_k^{cal}) / l_k \quad , \quad (4)$$

with  $f_{ki} = 1$  if ray  $k$  cross cell  $i$ , and  $f_{ki} = 0$  if it does not.

For every cell  $i$  crossed by rays,  $\Delta u_{ki}$  are summed and averaged by the number of crossings giving a slowness correction:

$$\Delta u_i^{cor} = \sum_{ii=1}^{X_i} (t_k^{obs} - t_k^{cal}) / l_k / X_i \quad , \quad (5)$$

$$X_i = \sum_{k=1}^M f_{ki} \quad , \quad (5a)$$

where  $X_i$  is the number of ray segments in cell  $i$ . Now the cell slownesses are updated:

$$u_i = u_i + \Delta u_i^{cor} \quad . \quad (6)$$

Then the procedure jumps back to Equation 3.

Back-projection of the differences  $(t_k^{obs} - t_k^{cal})$  between observed and calculated first arrival times is repeated in this way until the differences reach noise levels or until a set number of iterations is reached.

We note here the motivation for using iterative back-projection to estimate the slowness values that would fit the observed travel-times. The observed travel times  $t_k^{obs}$  can be written as a matrix equation:

$$\begin{matrix} t_1^{obs} \\ t_i^{obs} \\ t_M^{obs} \end{matrix} = \begin{bmatrix} \Delta l_{11} & \cdots & \Delta l_{1N} \\ \vdots & \ddots & \vdots \\ \Delta l_{M1} & \cdots & \Delta l_{MN} \end{bmatrix} * \begin{matrix} u_1 \\ u_j \\ u_N \end{matrix} \quad (7)$$

The  $u_j$  are the cell slownesses, and the  $\Delta l_{ij}$  are the lengths of ray  $i$  in cell  $j$ . Usually, many of the  $\Delta l_{ij}$  are zero and the number of cells  $N$  greatly exceeds the number of rays  $M$ . Furthermore, the equations may not be linearly independent. So, simple matrix inversion cannot be used to find the unknown slowness values  $u_j$ . The application of pseudo-inverses via SVD is an alternative method that may work. Iterative back-projection of arrival-time residuals is simpler and more straightforward than pseudo=inverses or other algebraic methods.

It needs to be proven that iterative back-projection is effective for finding good estimates of  $u_j$ . Likely, much depends on ray coverage and the distribution of ray angles spanning the scanned area.

## EXPERIMENTAL RESULTS

### Piezopin survey

We conducted a physically-modelled time-lapse seismic survey in a simulated marine environment. Figure 2(a) shows the positions of source and receiver transducers in the 2D region being scanned seismically. The complete scan consisted of 1333 transmission raypaths covering a 2D circular area. Figure 2(b) shows a selection of rays joining the sources and receivers.

Piezopin transducers were used as the source and receiver immersed in water. The source piezopin was driven by a 200V pulse. Receiver signals were amplified with a gain of 1000, sampled at 1ms intervals, and saved as common source gathers (CSGs) in SEG-Y files. Laboratory dimensions and times were scaled by 10,000 to yield geological world dimensions and times.

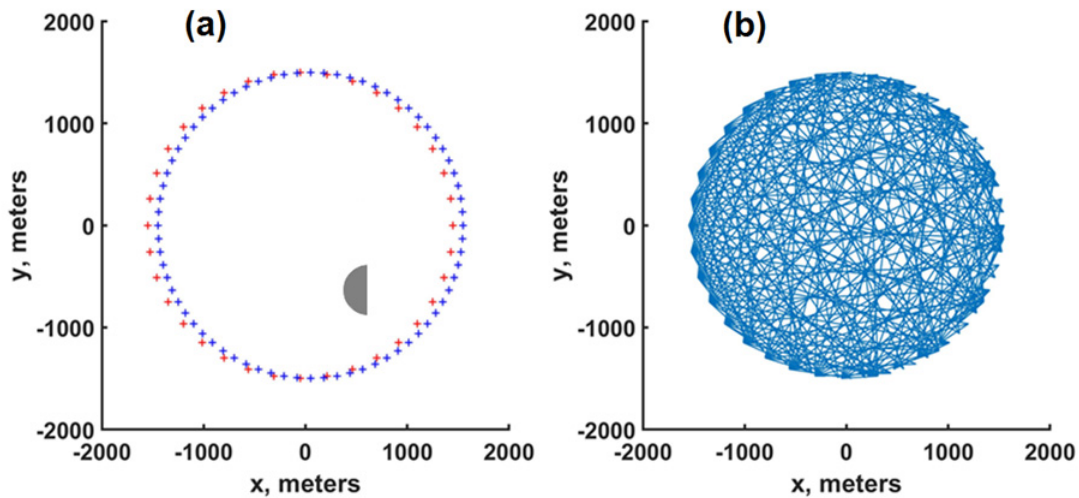


FIG. 2. (a) Positions in the 2D plane of source (red) and receiver (blue) transducers. A single target is in the area being scanned. (b) A selection of transmission raypaths crossing the scanned area. Only every 5<sup>th</sup> ray (out of 1333) is displayed.

We conducted two surveys using the piezopin transducers and the acquisition geometry shown on Figure 2. The first was done through only water within the scanned area. Figure 3 displays an example CSG from this initial scan. A second scan was then done after placing a PVC plastic target inside the scanned area (see Figure 2.). Figure 4 displays an example CSG from this second scan.

The arrival-time anomaly on Figure 4 is due to the presence of the target within the scanned area. We picked first-arrival times for all 1333 traces from both the first and second scans and used them as the input data into the iterative back-projection method outlined above (we made no assessment of the quality of the time picks). The resulting velocity images are shown on Figures 5 and 6.

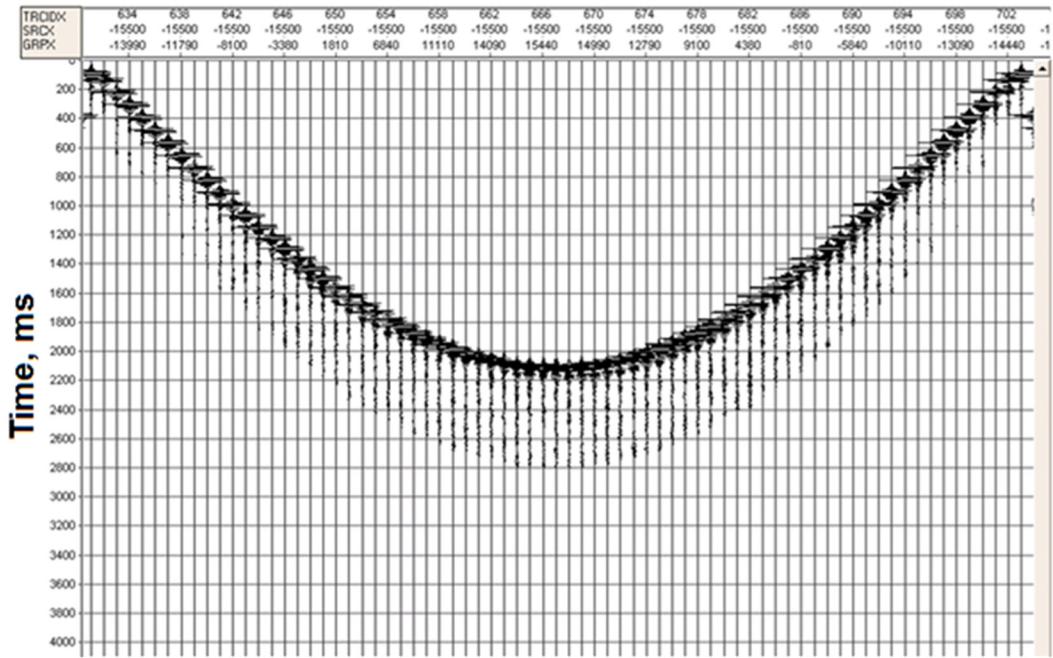


FIG. 3. (a) An example piezopin-acquired CSG from the baseline survey. There is no target within the scanned region. Wavelet frequencies are about 50Hz (500kHz unscaled).

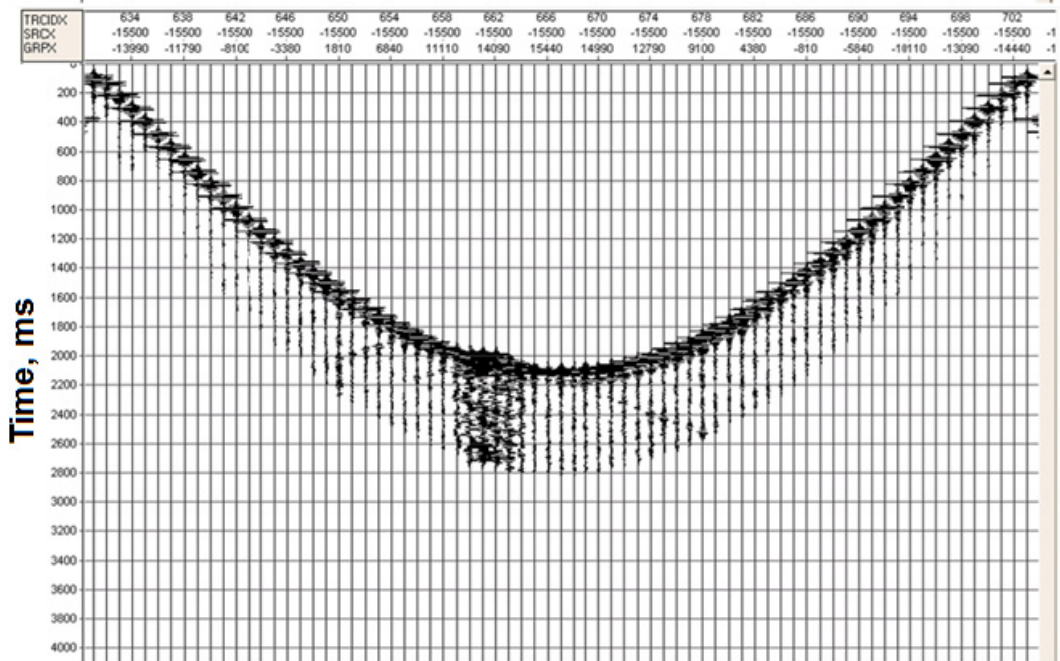


FIG. 4. Example piezopin-acquired CSG from the monitor survey. There is one target within the scanned region. Wavelet frequencies are about 50Hz (500kHz unscaled). Henley (2022, this volume) has used the full dataset in a shadow projection method to locate the target.

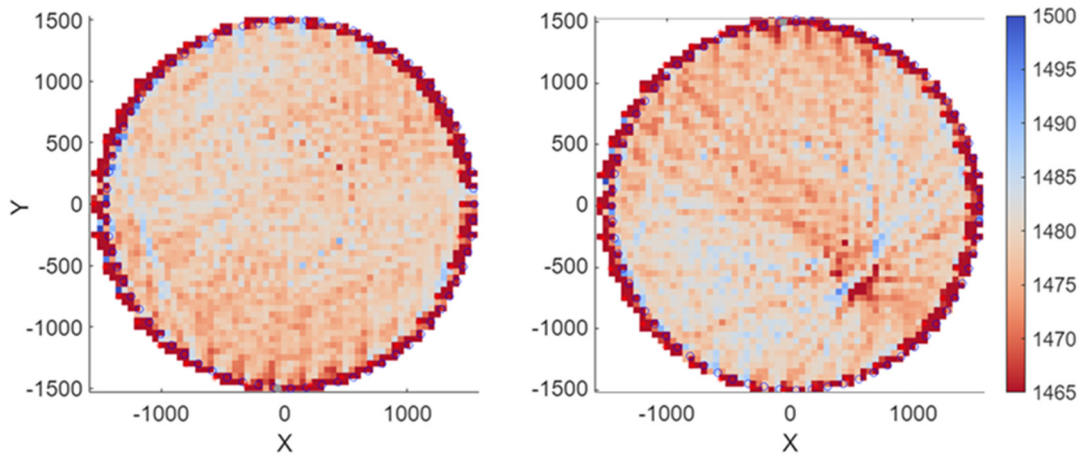


FIG. 5: Velocity images after **10 iterations**, for survey over area with no targets (left) and with one target (right).

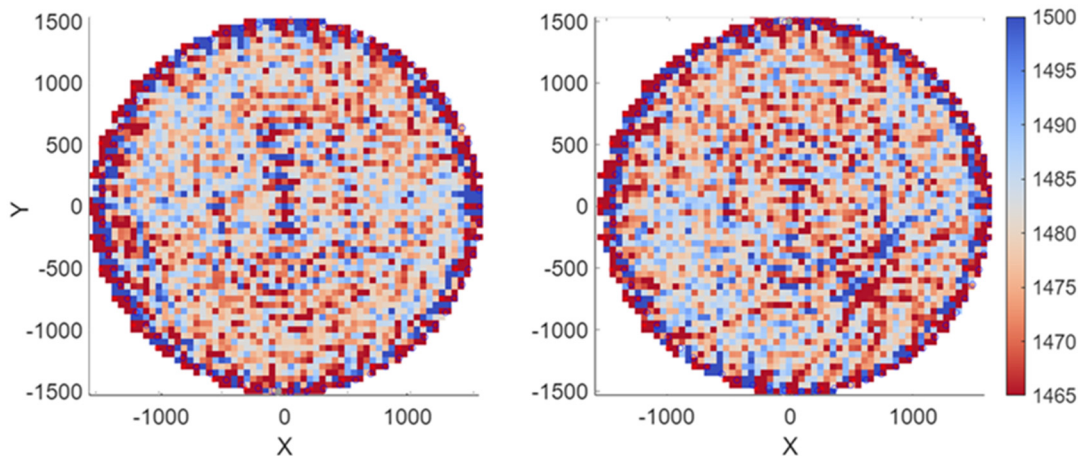


FIG. 6: Velocity images after **50 iterations**, for survey over area with no targets (left) and with one target (right). The speckled appearance of these images compared to those on Figure 4 is probably due to the extra iterations try to over fit to the noise in the input time picks.

### Time-lapse survey using buzzer transducers

We performed a physically-modelled time-lapse seismic survey in a simulated marine environment. Figure 7(a) shows the positions of source and receiver transducers in the 2D region being scanned seismically. The complete scan consisted of 2665 transmission raypaths covering a 2D circular area. Figure 7(b) shows a selection of rays joining the sources and receivers. The laboratory dimensions and times were scaled by 10,000 to yield geological world dimensions and times.

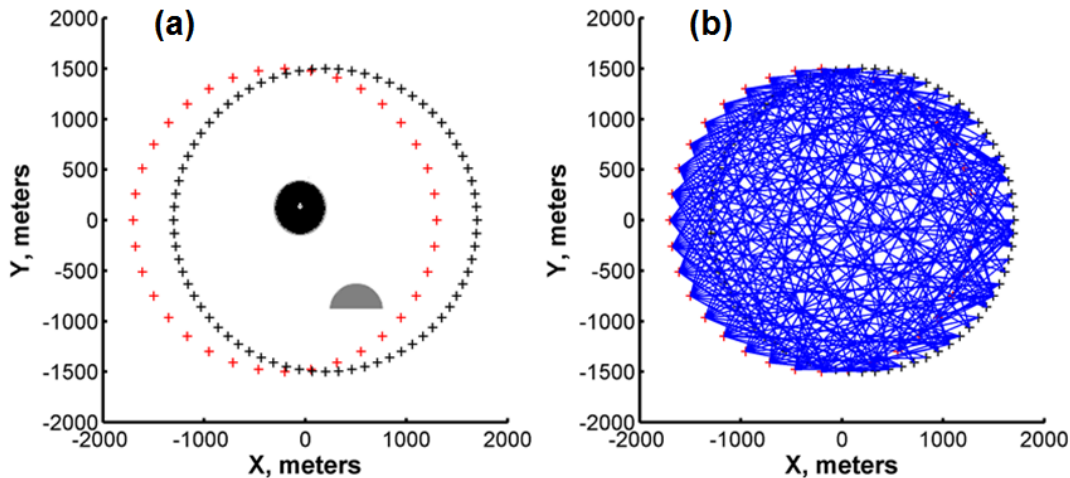


FIG. 7. (a) Positions in the 2D plane of source (red) and receiver (blue) transducers. Two isolated targets are in the area being scanned. (b) A selection of transmission raypaths crossing the scanned area. Only every 10<sup>th</sup> ray (out of 2665) is displayed.

Murata buzzer transducers were used as source and receiver. The source buzzer was driven by a 35V pulse. Receiver signals were amplified with a gain of 100, sampled at 2ms intervals, and saved as common source gathers (CSGs) in SEG-Y files. We mention parenthetically that the full datasets from these surveys were used by Keating et al. (2022, this volume) as input to FWI processing to obtain good images of the targets,

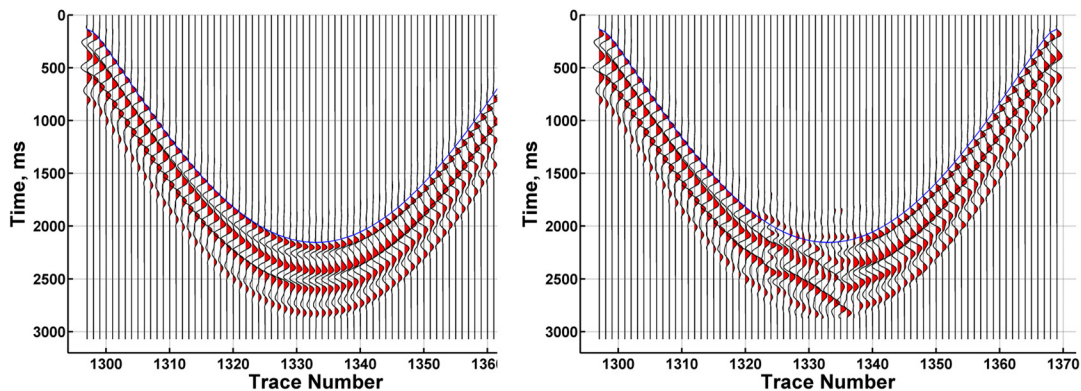


FIG. 8. Normalized-trace displays. Left: A CSG from the baseline survey. Right: A CSG from the monitor survey. The effect of the targets on the transmission seismograms is clearly seen.

Figure 8 plots example CSGs from the baseline and monitor surveys. The seismograms clearly indicate the presence of targets within the scanned area. Normalized traces are effective for emphasizing transmission arrival times; in this section we are interested in the relative amplitudes of arrivals. We therefore picked the maximum peak-to-peak amplitudes for all traces and expressed them in decibel units. In addition, for rays with identical source and receiver coordinates, we calculated the ratios of monitor amplitudes over baseline amplitudes. On Figure 9, we have plotted all three attributes for the traces on the example CSGs.

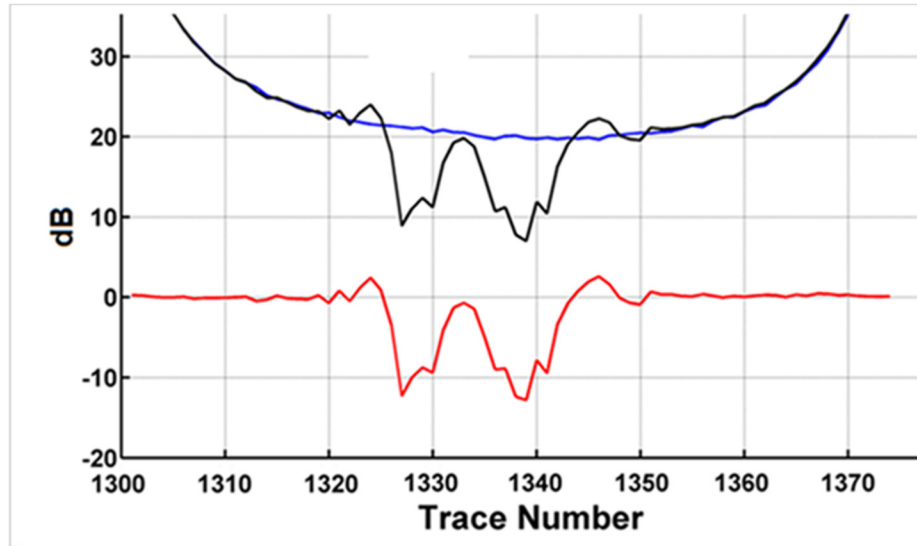


FIG. 9. Blue and black lines are maximum peak-to-peak amplitudes for the baseline and monitor CSGs above. Red line is the ratio of monitor survey amplitudes to baseline survey amplitudes.

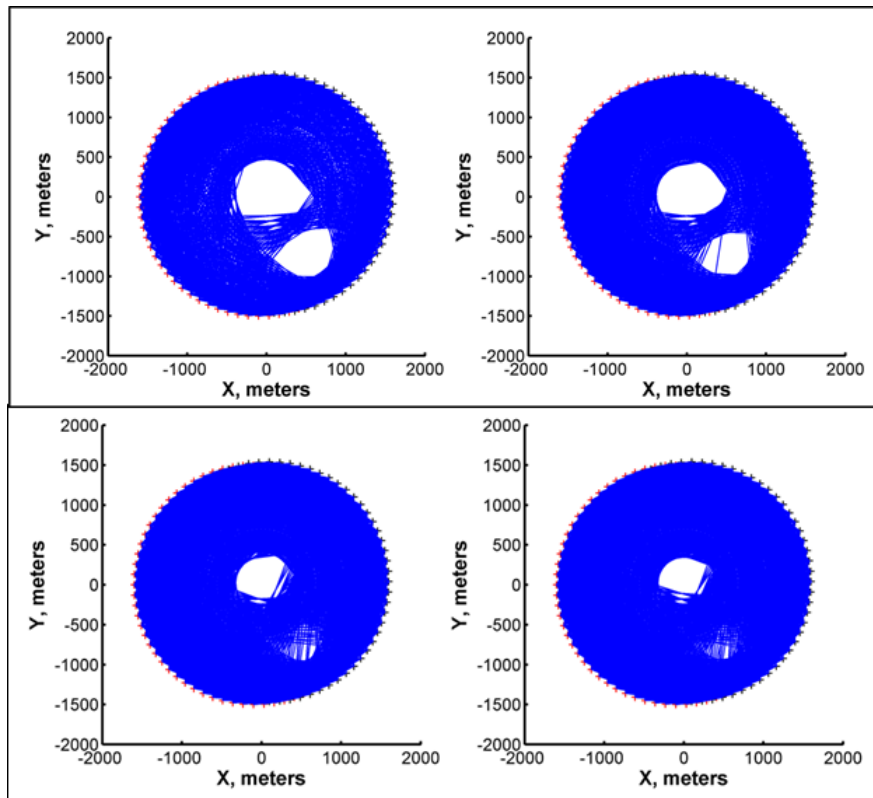


FIG. 10. A ray is drawn if the peak-to-peak amplitude ratio associated with it exceeds a cutoff threshold. Cutoff values for the top two images are 0dB and -1dB. Cutoff values for the bottom two images are -4dB and -5dB.

We offer the following remarks on the plots of amplitudes and their ratios. We see that some rays associated with the monitor survey have anomalous values. For those rays whose amplitudes are not anomalous (presumably because they have clear paths that do not intersect with targets), the amplitude ratios have values very close to 0dB. This means that measured amplitudes for such rays are almost perfectly repeatable in the monitor and baseline surveys.

We can use the amplitude ratios to achieve our goal of obtaining a rough estimate of the location, size, and shape of isolated targets within the scanned area. If the amplitude ratio associated with a given ray is above a certain cutoff value, we back-project or draw the ray, i.e., the ray is “visible”. Otherwise, the ray is not drawn. We treat all the rays in the monitor rays in this fashion.

Based on the amplitude ratios on Figure 9, we set cutoff values of 0dB, -1dB, -4dB, and -5dB to produce the “acoustic transparency” images shown Figure 10. In all four images, the approximate locations and sizes of the targets are revealed, although the shapes are not reliably defined. Even though the images vary somewhat as the cutoff value is changed, we feel they vindicate our belief that simple back-projection of arrival amplitudes can quickly define the approximate geometries of isolated targets.

## **DISCUSSION AND CONCLUSION**

In this work, the iterative back-projection of arrival-time residuals used on the piezopin data yielded disappointing results. There are three possible reasons for this:

- a) The picking of arrival times was inaccurate because the seismic traces were noisy (real-world seismic data may have SNRs as low as 1).
- b) The recorded source-receiver coordinates did not represent the actual physical locations accurately.
- c) Our implementation of the technique may not have been done properly.

The technique itself needs more validation, ideally using “perfect” seismic data generated numerically by finite-difference forward modelling.

The method of back-projecting “visible” rays based on amplitude ratios observed on baseline and monitor surveys was successful in quickly defining the rough locations and sizes of discrete isolated targets imbedded in a homogeneous medium. For more complex velocity-density structures the method may be less effective. An interesting question to answer experimentally is how many target of various sizes can be imaged in this way.

## **ACKNOWLEDGEMENT**

This work was funded by the industrial sponsors of CREWES), and by the NSERC grant CRDPJ 543578-19. WE express our gratitude for their support.

## **REFERENCES**

- Henley, D.C., 2022 (this volume), Shadow imaging attenuation projection of acoustic waves without arrival picking, CREWES Research Reports, **34**, 21.
- Keating, S., Innanen, K.A., and Wong, J., 2022 (this volume), Cross-gradient regularization for multiparameter FWI of physically modelled data, CREWES Research Reports, **34**, 30.